DX center formation in highly Si doped AlN nanowires revealed by trap assisted space-charge limited current

Rémy Vermeersch,[1,2,a)] (iD) Gwénolé Jacopin,[1] (iD) Bruno Daudin,[2] (iD) and Julien Pernot[1] (iD)

AFFILIATIONS

[1]University Grenoble Alpes, CNRS, Grenoble INP, Institut Néel, 38000 Grenoble, France
[2]University Grenoble Alpes, CEA, IRIG-PHELIQS, NPSC, 17 rue des martyrs, 38000 Grenoble, France

[a)]Author to whom correspondence should be addressed: remy.vermeersch@neel.cnrs.fr

ABSTRACT

Electrical properties of silicon doped AlN nanowires grown by plasma assisted molecular beam epitaxy were investigated by means of temperature dependent current–voltage measurements. Following an Ohmic regime for bias lower than 0.1 V, a transition to a space-charge limited regime occurred for higher bias. This transition appears to change with the doping level and is studied within the framework of the simplified theory of space-charge limited current assisted by traps. For the least doped samples, a single, doping independent trapping behavior is observed. For the most doped samples, an electron trap with an energy level around 150 meV below the conduction band is identified. The density of these traps increases with a Si doping level, consistent with a self-compensation mechanism reported in the literature. The results are in accordance with the presence of Si atoms that have three different configurations: one shallow state and two DX centers.

Wide bandgap nitride materials are of particular interest due to their applications as UV emitters and high-power or high-temperature electronic devices. Specifically, aluminum nitride (AlN) is a material of choice since it benefits from a large direct bandgap of 6.2 eV and a high breakdown field of around 10 MV/cm. Realization of these devices requires precise control of material crystallographic quality, carrier concentration, and conductivity of the layers over a wide range of doping levels from a few 10^{15} cm^{-3} to 10^{19} cm^{-3} in electronic and optoelectronic applications. Whereas considerable advances have been achieved in gallium nitride (GaN), silicon carbide, and diamond, AlN still suffers from limitations when doped with either Si (n-type) or Mg (p-type) restraining its electrical performances.

In pure AlN and AlGaN materials with an AlN mole fraction above 60%–80%, Si atoms no longer prefer to be in purely substitutional cation sites but will undergo a transition through lattice relaxation, preventing the impurity to act as a shallow *d* donor.[1–3] This so-called DX state is related to Si in an interstitial site and exhibits ionization energy much larger than 70 meV of Si$_{Al}$ evaluated from the hydrogenic model. Experimentally, a wide variety of donor ionization energy values are found depending on measurement techniques, ranging from $\sim$70 meV[4–7] to $\sim$300 meV.[7–10] The discussion supported by density functional theory calculations on the nature of the different Si states in AlN was initiated in the late 1990s and is still ongoing. However, no consensus appears on the Si configuration within the AlN lattice nor on its electronic state and transitions.[11–16] In addition, compensation of donors occurs for Si concentration as low as 10^{17} cm^{-3}, reducing even more the doping efficiency of Si in AlN.[17] Its origin arises from the presence of DX centers, which can be considered as acceptors as the following relation holds:[1,2,11]

$$2d^0 \leftrightarrow d^+ + DX^-, \tag{1}$$

where d^0 and d^+ are the neutral and positively ionized states of the shallow donor and DX$^-$ is the negatively charged DX state. The increasing compensation level with an increasing Si content also comes from an increasing amount of intrinsic impurities such as Al vacancies, Si$_N$, and V$_{Al}$–nSi$_{Al}$ (n = 1, 2, 3) complexes when the Fermi level approaches the conduction band (CB).[17,18] The combination of all these effects implies a drastic reduction in the electron concentration in AlN:Si leading to poor electrical conduction.

Recently, stabilization of the shallow state of Si impurity was demonstrated in the case of implanted layers annealed at relatively low temperatures.[19] Breckenridge and co-workers reported an ionization energy of 70 meV after annealing at 1200 °C while a 270 meV

ionization energy was found for samples annealed at higher temperatures. In a previous article, we reported the presence of shallow Si states in AlN nanowires (NWs) with an ionization energy of 75 meV.[20] Such states dominate the electrical conduction at room temperature for NWs in the low Si flux range whereas at a higher Si flux, it is no longer the case. In relation with such an increase, the effect of Fermi level pinning on lateral NW sidewalls was discussed as it can drastically affect electrical properties.[21] In addition to the presence of shallow states, the controversial issue of DX formation with higher ionization energies in the 100–300 meV range still needs to be clarified. Accordingly, the present article focuses on the role of the DX complexes as trapping centers for electrons in Si-doped AlN NWs, which can be studied in the framework of the space-charge limited current (SCLC) theory.

As described by Lampert,[22] the simplified theory of SCLC is designed in order to model current flow in insulator containing traps based on Poisson's equation and the charge neutrality equation at quasi-thermal equilibrium. The case of a material with free electron concentration n containing a single trap with concentration N_t located within the forbidden gap at a single energy level above the Fermi level and a homogenous electronic transport is hereafter considered. At low bias, Ohmic conduction occurs thanks to the drift of charge carriers present at thermodynamic equilibrium, following Ohm's law:

$$I_\Omega = \frac{en\mu SV}{a},\qquad(2)$$

where e is the electronic charge, μ is the mobility, V is the applied voltage between the anode and cathode separated by distance a, and S is the contact surface. Depending on the trap nature and its energy position with respect to the Fermi level, a number of them can be charged close to the contact, repulsing carriers and preventing their direct injection from the contact. In the case of deep traps, a certain voltage threshold is needed to overcome this repulsion, which is equal to $V_{TFL} = \frac{ea^2}{2\varepsilon}N_t$, with ε being the dielectric constant of the material. In the case of nanowires with high surface/volume ratio, V_{TFL} may be significantly reduced due to poor electrostatic screening.[23] Once this voltage is reached, the current flow arises from injected carriers at the contact resulting in a steep increase in current, sometimes wrongly assigned to impact ionization.[24] Starting from V_{TFL} and for higher voltages, the current follows Child's law and is only dependent on the carrier mobility in the band, μ, but no longer on the density n of electrons present in the material

$$I_C = \frac{8e\varepsilon\mu SV^2}{9a^3}.\qquad(3)$$

However, in the case of shallow traps, and as the Fermi level lies below the trap level close to the anode, only a fraction might be already neutralized. Accordingly, direct injection from the contact can occur at voltages lower than V_{TFL}, ensuing the onset of Child's law at a voltage, $V_{\Omega-\theta} = \frac{ea^2}{2\varepsilon\theta}n$. Here, the free/trapped carrier ratio θ is defined by the following equation:

$$\theta = \frac{N_C}{N_t}\exp\left(-\frac{E_C - E_t}{kT}\right),\qquad(4)$$

with N_C being the effective density of state of the conduction band, k being Boltzmann's constant, T being the temperature, and $E_C - E_t$ being the relative position of the trap level with respect to the conduction band. This ratio, smaller than unity, is independent of the applied voltage. For $V_{\Omega-\theta} < V < V_{TFL}$, the current flows following Child's law corrected from θ smaller than 1,

$$I_C = \frac{8e\varepsilon\mu\theta SV^2}{9a^3}.\qquad(5)$$

In the case of $V \approx V_{TFL}$, filling of all traps occurs, and the current flows in standard Child's law regime with $\theta = 1$.

Samples under study were grown by PA-MBE under nitrogen-rich conditions on a low resistivity n-type Si (111) wafer. After the growth of a 350 nm Si-doped GaN stem, a Si-doped AlN section of around 450 nm was grown and capped by a 20 nm Si-doped GaN section. In all samples, GaN sections are doped with the same Si flux corresponding to $\sim 2 \times 10^{20}$ Si/cm^3 measured by energy dispersive x-ray spectroscopy (EDX). The silicon cell temperature (T_{Si}) was varied from sample to sample during the AlN section growth, ranging from 750 °C to 1300 °C. The silicon concentration in AlN was also measured by EDX and was ranging from a few 10^{15} Si/cm^3 to 6 $\times 10^{20}$ Si/cm^3. Widening and shortening of the NWs were observed at $T_{Si} > 1100$ °C assigned to an enhancement of adatom diffusion on lateral m-planes of the wires, consistent with previous observations.[25,26] Eventually, two populations of samples can be distinguished: a first one for $T_{Si} < 1200$ °C with a diameter of 80 and 810 nm long, a second one for $T_{Si} > 1100$ °C with a diameter of 130 nm and a length of 720 nm. It is worth noting that these dimensions are large enough to discard the effect of free carrier quantum confinement in NWs, supporting the assumption that the band structure is the same as in bulk. More details on NW growth and morphology can be found in Ref. 20. The description of the investigated samples is given in Table I.

In order to study the electronic transport properties of the AlN:Si NWs, samples were processed by optical lithography. $100 \times 100\ \mu m^2$ squared pads of Ti/Al (30/70 nm) were deposited on top of the NWs as a top contact. The highly conductive n-type (111)-Si substrate was used as a bottom contact. Electrical characterizations were carried out using two probes current–voltage (I–V) measurements. Contact resistances were assumed to be of limited influence on the measurements and negligible compared to the resistance of the n-AlN section, thanks to the metallic behavior[26] of the highly conductive n-GaN sections. To avoid self-heating due to high electrical power at large bias, the pulsed voltage was used with a ON state duration of 50 μs and a duty cycle of 2%. Figure 1(a) presents the results of current voltage measurements of several samples while Fig. 1(b) shows the coefficient m of the power law $I = V^m$, defined by

$$m = \frac{d(\log(I))}{d(\log(V))}.\qquad(6)$$

At lower bias (V <0.1 V), a linear regime corresponding to Ohmic behavior is observed, which has been extensively discussed in Ref. 20. At higher bias, this linear regime evolves toward a space-charge limited regime. Two behaviors can be distinguished depending on the doping level. For the lowest doped samples ([Si] $< 5 \times 10^{18}$ cm^{-3}), the transition is associated with a m value reaching more than 3 at voltages around 1 V. Following the transition regime, a quadratic behavior is observed. For the most doped samples ([Si] $> 1 \times 10^{19}$ cm^{-3}), the transition from $m = 1$ to $m = 2$ is monotonous and smooth. For S1200 and S1250, m reaches a value of 2 in a range of a few volts for

TABLE I. Description of studied samples. [Reproduced with permission from Vermeersch et al., Appl. Phys. Lett. **119**, 262105 (2021). Copyright 2021 AIP Publishing LLC.]

Sample name	T_{Si} (°C)	[Si] (cm^{-3})	NW diameter (nm)	NW length (nm)
S0	No Si	No Si	79	860
S750	750	2.4×10^{15}	81	815
S800	800	1.7×10^{15}	79	822
S850	850	1.0×10^{16}	79	815
S870	870	2.2×10^{16}	80	804
S900	900	5.2×10^{16}	75	828
S930	930	1.3×10^{17}	79	828
S1000	1000	9.5×10^{17}	79	815
S1050	1050	3.4×10^{18}	82	805
S1100	1100	9.4×10^{18}	89	767
S1200	1200	6.5×10^{19}	125	722
S1250	1250	2.0×10^{20}	126	700
S1300	1300	6.0×10^{20}	128	730

which Child's law regime is obeyed before increasing sharply above 10 V while it increases for a voltage as low as 4 V in S1300.

These observations are consistent with the theory of SCLC as formalized hereabove following Ref. 22. The different behaviors between the first and second NW population can be explained by assuming different trap characteristics (i.e., the energy level or concentration). In the case of the first population, the high m value extracted at ∼1 V is assigned to the trap filling limit, followed by a $I \propto V^2$ corresponding to Child's law regime. Equation (3) is used to fit the I–V curve, taking $S = 10^{-4}$ cm^{-2}, $a = 450$ nm, $\varepsilon = 9\varepsilon_0$,[27] and $\theta = 1$, leading to an electron mobility value around 0.01 cm^2/(V s) for almost all samples with [Si] $< 10^{19}$ cm^{-3}. Only S900 and S930 exhibit the mobility of 0.8 and 0.08 cm^2/(V s), respectively. These values are surprisingly low compared to values reported in the literature in the case of bulk
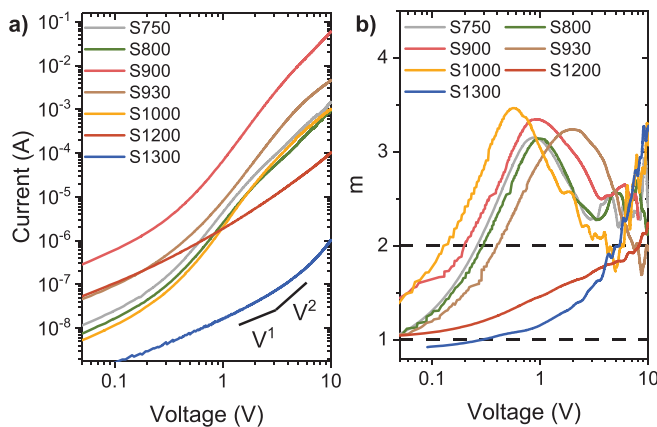
a)
b)

FIG. 1. (a) Current voltage (I–V) characteristic of several samples. (b) Plot of $m = \frac{d(\log(I))}{d(\log(V))}$ vs voltage for different samples. Horizontal dashed lines are guides for the eye.

materials.[8,28] One explanation could arise from the overestimation of the conduction area S under consideration. Indeed, part of an individual wire can be depleted due to Fermi level pinning on the NW sidewall. Additionally, a certain amount of NWs within the probed array may not contribute to the current flow due to height or diameter inhomogeneities.

As shown in Fig. 1(b), the slope increase from 1 to 2, for the most doped samples, indicates the predominance of a trap filling regime. This difference in behavior between low and high doping could arise from either a drastic increase in the trap density or the formation of a new trap located above Fermi level. Conversely, the Ohmic regime observed for those samples points toward a conduction exclusively related to the DX state.[20] Thus, it highlights a correlation between the increase in Si doping and the DX concentration and the apparition of a regime of trap filling in the line of other studies.[7,10]

In order to further characterize the trapping behavior in AlN:Si NWs, temperature dependent current-voltage measurements were carried out between 200 and 500 K. I–V characteristics for S870 and S1250 are presented in Fig. 2. The behavior at lower bias in the Ohmic regime is consistent with the ionization of carriers with temperature. At higher bias, the contrast between the two samples emphasizes the difference in trap population previously highlighted. Almost no temperature dependence is found for the low doped samples in agreement with a trap filled space-charged limited regime. In this regime, Eq. (5) with $\theta = 1$ holds, in which the only temperature dependent term is the mobility, expected not to vary on several orders on magnitude.[8] In the case of S1250, a clear temperature dependence is seen in the V^2 regime, which is consistent with the trap filling mechanism and the θ dependence with temperature [Eq. (4)].

Fitting the quadratic region with modified Child's law function [Eq. (5)], the quantity $\theta\mu S$ was extracted. Considering N_C to vary as $N_C = N_C^0 T^{\frac{3}{2}}$, Eq. (4) is rewritten as

$$\theta\mu S T^{-\frac{3}{2}} = \frac{\mu S N_C^0}{N_t} \exp\left(-\frac{E_C - E_t}{kT}\right). \quad (7)$$

Figure 3 shows the evolution of the quantity $\theta\mu S T^{-\frac{3}{2}}$ as a function of 1000/T in a semi-logarithmic scale. Assuming no variation of mobility with temperature,[8] $E_C - E_t$ values equal to 162, 144, and 132 meV were extracted for S1200, S1250, and S1300, respectively. Taking a mobility of 0.01 cm^2/(V s) and a surface of 100×100 μm^2, fitting of S1250 gives a trap density of 1.1×10^{20} cm^{-3} to be compared with [Si] $= 2 \times 10^{20}$ cm^{-3} in this sample, measured by EDX. As extracted from study of the Ohmic regime, the main donor exhibits an ionization energy of 270 meV (Ref. 20) designated as the transition level energy of DX centers. Interestingly, the trap is found to be at around 150 meV and, therefore, shallower than the DX state at 270 meV. Moreover, with the increase in the Si flux, an increasing proportion of trap with respect to [Si] is measured. This cannot be compatible with a two levels system in which Si is either in a shallow substitutional state or in a DX state but rather suggests the implication of a third Si-related state. Although the presence of defects, such as V_{Al}–Si_{Al} complexes, cannot be discarded, the ionization energy of such complexes is not in agreement with our experimental data.[17] By contrast, our results are consistent with Ref. 16, who proposed two metastable configurations of Si in AlN, perpendicular to and along the c-axis, denoted DX_c and DX_a, respectively. Their transition energy levels of around 170 and 230 meV, respectively, are in line with our results, suggesting that
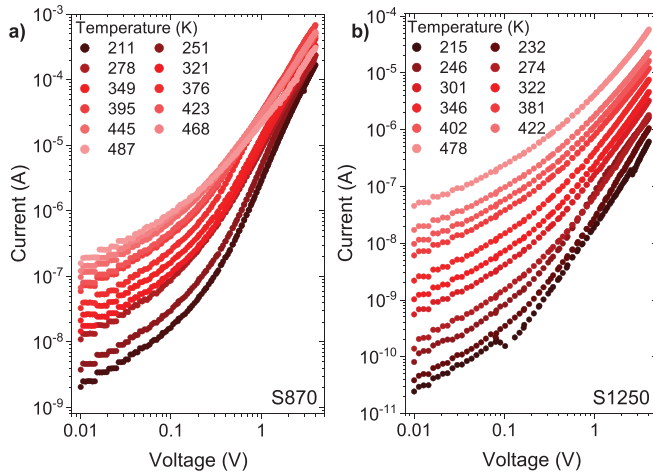
FIG. 2. I–V characteristics for different temperatures for (a) S870 and (b) S1250.

the trap level identified at ∼150 meV indeed corresponds to a second DX center. However, it is worth stressing that other published works based on the DFT provide a wide variety of DX states and ionization energies.[1,11,12,29] More generally, those three levels were identified both experimentally and by calculations. However, they were never observed in the same sample set.

Thereafter, we assume that this trap with a transition level energy of 150 meV is a DX center, denoted DX_1. The deeper state at 270 meV will be denoted DX_2. First, one can postulate that the configurations of Si atoms can be either shallow d or one of the two DX_1 and DX_2 centers, leading to the equation

$$[\text{Si}] = [d] + [DX_1] + [DX_2]. \qquad (8)$$

Second, in the lowest doped sample, d states participate in the Ohmic conduction, DX_2 centers appear only at higher temperatures, and
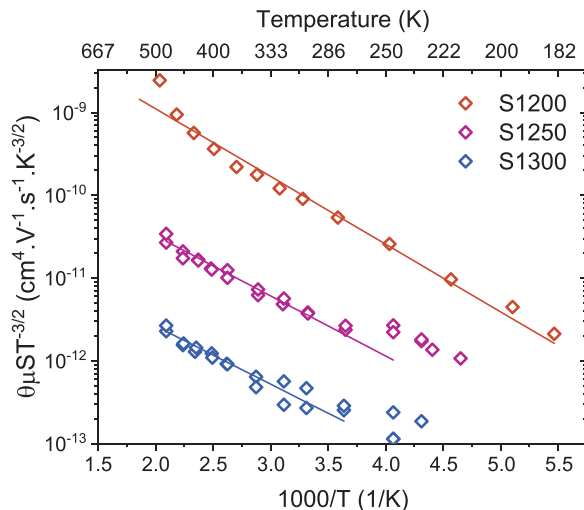
no thermal activation of DX_1 is observed. Hence, we can write: $[d] > [DX_1] + [DX_2]$. In other words, part of shallow donors is not involved in DX formation, no self-compensation occurs for those ones, and they can be ionized with a 70 meV ionization energy to deliver electrons to the conduction band.

On the other hand, in the most doped samples, all d and DX_1 states are depleted, and so positively charged, i.e., in a d^+ and neutral DX_1^0 state, respectively, while DX_2 are shared between neutral DX_2^0 and negatively DX_2^- charged states. This results from the fact that only the DX_2 transition energy of 270 meV is measured by conductivity temperature dependence while the DX_1 transition energy of 150 meV is exclusively put in evidence as an electron trap during trap assisted SCLC measurement.[30]

Such a situation indicates that an additional acceptor N_a must be lying within the bandgap to compensate Si donors. Aluminum vacancies (V_{Al}) formation is predicted to be favored in n-type AlN. They could play this role by compensating DX centers as several studies reported.[17,31] When introducing this acceptor in our model and in the specific case of these highly doped samples, the following relationship can be written:

$$[d^+] + [DX_1^-] + [DX_2^-] > [N_a^+] > [d^+] + [DX_1^-]. \qquad (9)$$

The large amount of depleted states is indeed in agreement with the low mobility values previously discussed, regardless of the sample.

Transition level energies of Si in AlN from this study and literature are gathered and plotted vs silicon concentration in Fig. 4. In contrast to the present study, all samples were bulk AlN grown by different techniques on various substrate materials. Three distinct families of ionization energies emerge corresponding to the ones reported in the present report: 75, 150, and 270 meV. As these three levels are only observed in the AlN NWs, it suggests that their relative population could depend on both the doping level and growth technique. It further suggests that NW morphology and peculiar strain relaxation mechanisms could favor the formation of a full set of possible Si-related DX centers. Especially, a level at ∼160 meV below CB was predicted by several computational studies[11,13,16] but not often measured experimentally. It must be noticed that because the substitutional d level is quite shallow and its ionization energy is well described by the

FIG. 3. Evolution of $\theta\mu ST^{-\frac{3}{2}}$ as a function of 1000/T for S1200, S1250, and S1300. Straight lines are exponential fits.
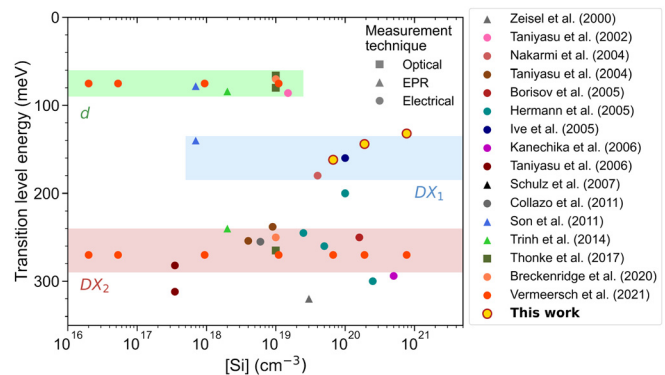

FIG. 4. Review of transition level energies of silicon in AlN reported in the literature as a function of the silicon concentration. Optical refers to photoluminescence techniques, EPR to electron paramagnetic resonance and electrical refers to either Hall or conductivity measurements. Green, blue, and red regions are indicative.

hydrogenic model, one can evaluate the metal nonmetal transition to be in the range of $\sim 10^{19} \, \mathrm{cm}^{-3}$, as observed for other wide bandgap semiconductors ($\sim 10^{19} \, \mathrm{cm}^{-3}$ in N-doped 4H-SiC[32] or $\sim 10^{18} \, \mathrm{cm}^{-3}$ in Si-doped GaN[33]). However, in Fig. 4, no ionization energy decrease vs Si-doping concentration is observed at around $\sim 10^{19} \, \mathrm{cm}^{-3}$. Instead, the abrupt appearance of the DX_1 level and the simultaneous disappearance of the d level are put in evidence.

Understanding the mechanisms by which n-type AlN can be doped with Si is essential for the realization of efficient deep UV light-emitting diodes or ultra-wide bandgap devices for power electronics. In this work, Si-doped AlN NWs were characterized using current-voltage measurements. The increase in the Si flux resulting in an increased DX center concentration is shown to govern the electrical characteristics. The theory of space-charge limited current assisted by traps was used in order to understand differences in conduction behaviors. Especially, the apparition of a second Si-related level is revealed, and its position within the bandgap was estimated around 150 meV below the conduction band, which was assigned to a second DX state. Finally, three Si configurations were demonstrated, namely, a shallow donor and two DX centers, in accordance with results from the literature.

AUTHOR DECLARATIONS
Conflict of Interest

The authors have no conflicts to disclose.

DATA AVAILABILITY

The data that support the findings of this study are available from the corresponding author upon reasonable request.

REFERENCES

[1]P. Bogusławski and J. Bernholc, Phys. Rev. B **56**, 9496 (1997).
[2]C. Park and D. Chadi, Phys. Rev. B **55**, 12995 (1997).
[3]P. Pampili and P. J. Parbrook, Mater. Sci. Semicond. Process. **62**, 180 (2017).
[4]B. Neuschl, K. Thonke, M. Feneberg, R. Goldhahn, T. Wunderer, Z. Yang, N. M. Johnson, J. Xie, S. Mita, A. Rice, R. Collazo, and Z. Sitar, Appl. Phys. Lett. **103**, 122105 (2013).
[5]K. Thonke, M. Lamprecht, R. Collazo, and Z. Sitar, Phys. Status Solidi A **214**, 1600749 (2017).
[6]N. T. Son, M. Bickermann, and E. Janzén, Appl. Phys. Lett. **98**, 092104 (2011).
[7]R. Zeisel, M. Bayerl, S. Goennenwein, R. Dimitrov, O. Ambacher, M. Brandt, and M. Stutzmann, Phys. Rev. B **61**, R16283 (2000).
[8]Y. Taniyasu, M. Kasu, and T. Makimoto, Appl. Phys. Lett. **85**, 4672 (2004).
[9]M. Hermann, F. Furtmayr, A. Bergmaier, G. Dollinger, M. Stutzmann, and M. Eickhoff, Appl. Phys. Lett. **86**, 192108 (2005).
[10]S. Goennenwein, R. Zeisel, O. Ambacher, M. S. Brandt, M. Stutzmann, and S. Baldovino, Appl. Phys. Lett. **79**, 2396 (2001).
[11]L. Gordon, J. L. Lyons, A. Janotti, and C. G. Van De Walle, Phys. Rev. B **89**, 085204 (2014).
[12]L. Silvestri, K. Dunn, S. Prawer, and F. Ladouceur, Appl. Phys. Lett. **99**, 122109 (2011).
[13]L. Silvestri, K. Dunn, S. Prawer, and F. Ladouceur, Europhys. Lett. **98**, 36003 (2012).
[14]P. Bogusławski, E. L. Briggs, and J. Bernholc, Appl. Phys. Lett. **69**, 233 (1996).
[15]C. G. Van de Walle, Phys. Rev. B **57**, R2033 (1998).
[16]I. A. Aleksandrov and K. S. Zhuravlev, J. Phys. **32**, 435501 (2020).
[17]J. S. Harris, J. N. Baker, B. E. Gaddy, I. Bryan, Z. Bryan, K. J. Mirrielees, P. Reddy, R. Collazo, Z. Sitar, and D. L. Irving, Appl. Phys. Lett. **112**, 152101 (2018).
[18]C. G. Van de Walle, J. Neugebauer, C. Stampfl, M. D. McCluskey, and N. M. Johnson, Acta Phys. Pol., Ser. A **96**, 613 (1999).
[19]M. Hayden Breckenridge, Q. Guo, A. Klump, B. Sarkar, Y. Guan, J. Tweedie, R. Kirste, S. Mita, P. Reddy, R. Collazo, and Z. Sitar, Appl. Phys. Lett. **116**, 172103 (2020).
[20]R. Vermeersch, E. Robin, A. Cros, G. Jacopin, B. Daudin, and J. Pernot, Appl. Phys. Lett. **119**, 262105 (2021).
[21]R. Calarco, T. Stoica, O. Brandt, and L. Geelhaar, J. Mater. Res. **26**, 2157 (2011).
[22]M. A. Lampert, Phys. Rev. **103**, 1648 (1956).
[23]A. A. Talin, F. Léonard, B. S. Swartzentruber, X. Wang, and S. D. Hersee, Phys. Rev. Lett. **101**, 076802 (2008).
[24]A. Rose, Phys. Rev. **97**, 1538 (1955).
[25]F. Furtmayr, M. Vielemeyer, M. Stutzmann, J. Arbiol, S. Estradé, F. Peiró, J. R. Morante, and M. Eickhoff, J. Appl. Phys. **104**, 074309 (2008).
[26]Z. Fang, E. Robin, E. Rozas-Jiménez, A. Cros, F. Donatini, N. Mollard, J. Pernot, and B. Daudin, Nano Lett. **15**, 6794 (2015).
[27]J. S. Thorp, D. Evans, M. Al-Naief, and M. Akhtaruzzaman, J. Mater. Sci. **25**, 4965 (1990).
[28]Y. Taniyasu, M. Kasu, and T. Makimoto, Appl. Phys. Lett. **89**, 182112 (2006).
[29]J. B. Varley, A. Janotti, and C. G. Van De Walle, Phys. Rev. B **93**, 161201(R) (2016).
[30]Because Compensation Hydrogen State D^{+} is too close to conduct band, equation based Boltzmann's distribution is no more valid trap fill. Regime tends to trap free regime as shown Ref. 22.
[31]C. Stampfl and C. G. Van de Walle, Phys. Rev. B. **65**, 1552121 (2002).
[32]A. Ferreira Da Silva, J. Pernot, S. Contreras, B. E. Sernelius, C. Persson, and J. Camassel, Phys. Rev. B. **74**, 245201 (2006).
[33]A. Wolos, Z. Wilamowski, M. Piersa, W. Strupinski, B. Lucznik, I. Grzegory, and S. Porowski, Phys. Rev. B. **83**, 165206 (2011).